Contents lists available at ScienceDirect

# Applied Catalysis B: Environmental

# $Cu/Al_2O_3$ catalysts for soot oxidation: Copper loading effect

F.E. López-Suárez, A. Bueno-López *, M.J. Illán-Gómez.

Inorganic Chemistry Department, University of Alicante. Ap. 99, E-03080 Alicante, Spain

ARTICLE INFO

ABSTRACT

$Cu/Al_2O_3$ catalysts with metal loading from 0.64 to 8.8 wt.% have been prepared and characterized by different techniques: $N_2$ adsorption at $-196\ ^{\circ}C$ (BET surface area), ICP (Cu loading), XRD, selective copper surface oxidation with $N_2O$ (Cu dispersion), TPR-$H_2$ (redox properties), and XPS (copper surface species). The catalytic activity for soot oxidation has been tested both in air and $NO_x/O_2$. The activity in air depends on the amount of easily-reduced Cu(II) species, which are reduced around $275\ ^{\circ}C$ under TPR-$H_2$ conditions. The amount of the most active Cu(II) species increases with the copper loading from Cu_1% to Cu_5% and remains almost constant for higher copper loading. In the presence of $NO_x$, the first step of the mechanism is NO oxidation to $NO_2$, and the catalytic activity for this reaction depends on the copper loading. For catalysts with copper loading between Cu_1% and Cu_5%, the catalytic activity for soot oxidation in the presence of $NO_x$ depends on $NO_2$ formation. For catalysts with higher copper loading this trend is not followed because of the low reactivity of model soot at the temperature of maximum $NO_2$ production. Regardless the copper loading, all the catalysts improve the selectivity towards $CO_2$ formation as soot oxidation product both under air and $NO_x/O_2$.

© 2008 Elsevier B.V. All rights reserved.

## 1. Introduction

Among the different catalytic after-treatment technologies proposed for soot removal in diesel exhausts, the so-called CRT (Continuously Regenerating Trap) seems to be the most satisfactory at this moment [1], especially for heavy-duty diesel applications. This system consists of a Pt catalyst for NO oxidation to $NO_2$, which is more oxidizing than NO and $O_2$. The soot filter located downstream is continuously regenerated by soot oxidation to $CO_2$ using the previously produced $NO_2$.

However, the CRT system presents several drawbacks that need improvements, motivating fundamental and applied research work. $NO_x$ removal over a CRT catalyst is somewhat less than 10% [1], and an additional system for $NO_x$ removal is required. It is also reported that soot oxidation is strongly inhibited by the presence of $SO_2$, so the CRT technology could not be introduced until low sulphur diesel fuel became available [1]. In addition, because of the high price of noble metals new active components based on non-noble metals are desired.

Looking for new, cheaper and efficient catalytic components [2], several alkali (Na, K, and Rb), alkali-earth (Ca), transition (Fe, Co, Ni, Cu, Cr, and Zr) and rare-earth (Ce) metals were loaded on

carbonaceous materials and the catalytic combustion was tested under $NO_x/O_2$. Among the metals studied, the lowest light-off temperatures were obtained with Rb and Cu [2]. In the same line, Bloom et al. [3] compared Fe, Cu and Ce fuel additives and found that only copper could efficiently regenerate the filter. Mul et al. [4] also screened a number of metal chlorides (Ba, Ca, Fe, Bi, Hg, Co, Mo, Ni, Cu, and Pb) for catalytic oxidation of model soot, concluding that those based on Pb and Cu are the most active. However, they reported that the application of metal chlorides as catalysts for diesel soot oxidation is questionable, because the loss of activity by evaporation or decomposition of the active species is a severe problem [4].

A number of copper-containing multi-component catalysts have also demonstrated to be active for soot oxidation, such us $CuO/CeO_2$ [5], copper-loaded MFI zeolite [6], $Al_2O_3$-[7] and $CeO_2$-[8] supported copper vanadates, $CuO/Nb_2O_5/SiO_2$-$Al_2O_3$ [9], copper-containing perovskites ($La_{0.8}K_{0.2}Cu_{0.05}Mn_{0.95}O_3$ [10] and $La_{0.8}Sr_{0.2}Mn_{0.5}Cu_{0.5}O_3$ [11]) and bimetallic Cu/K active phases supported on $ZrO_2$ [12], $Al_2O_3$ [13] and beta zeolite [14], among others.

The lower price of copper in comparison to noble metals makes this transition metal a promising candidate for practical utilization in diesel soot removal. Some authors have also reported that certain copper-containing catalysts ($La_{0.8}K_{0.2}Cu_xMn_{1-x}O_3$ [10], Cu/K/$Al_2O_3$ [13] and Cu/K/beta zeolite [14]) are able to promote the simultaneous removal of $NO_x$ and soot. Sulphur resistance seems

---

* Corresponding author.
E-mail address: agus@ua.es (A. Bueno-López).

to be another benefit of copper catalysts, since Mosconi et al. [15] have observed that a $Cu/Al_2O_3$ catalyst tested for soot oxidation under $NO_x/O_2$ does not suffer deactivation by $SO_2$ poisoning, even under severe conditions such as 1000 ppm $SO_2/600$ °C.

There have been proposed two main mechanisms through a metal oxide-catalysed soot oxidation could proceed [4], and both could be valid for copper catalysts. One of them is the reduction/oxidation mechanism (Mars and van Krevelen), where in a first step the metal oxide is reduced by the soot, and in a second step the catalyst is reoxidised by an oxidising gas. The other mechanism is based on a spill-over effect. Oxygen is activated on the surface of a metal oxide, and subsequently transferred to the soot surface where reacts yielding surface oxygen complexes and finally CO and/or $CO_2$. Mul et al. [4] reported that soot oxidation in air catalysed by copper chlorides is based on the latter mechanism. However, the catalytic combustion of copper-loaded char in $NO_x/O_2$ could be explained according to the reduction/oxidation mechanism, as suggest by the XPS analyses of the copper species (including $Cu(0)$, $Cu(I)$ and $Cu(II)$) detected on fresh and used samples [16]. In both cases, and also considering some other reported studies, it can be concluded that the redox properties of copper play a major role in its catalytic activity for carbon materials oxidation. However, there are several issues that remain unclear, such as the importance of the copper loading and dispersion in the activity of copper catalysts for soot oxidation and/or the relative importance of these two variables in comparison to the redox properties of this metal.

In the case of multi-component catalysts, the role of copper is more difficult to be analysed, and depends on the material considered. As an example, the role of copper on the catalyst $La_{0.8}K_{0.2}Cu_{0.05}Mn_{0.95}O_3$ [10], with perovskite structure, is proposed to be the creation of crystal defects. For copper-vanadium-cerium oxide catalysts, its high activity for model soot oxidation was attributed to the presence of the $V_2O_5$ phase, while it is suggested that copper (II) species are responsible for the low CO production [8].

In the current study, a set of $Cu/Al_2O_3$ catalysts with different metal loading, have been prepared, characterized and tested for soot oxidation both in air and $NO_x/O_2$. The goal of the study is to get insight into the properties of copper that could affect the catalytic activity, including copper loading, copper dispersion, type of surface copper species and copper redox properties.

## 2. Experimental

### 2.1. Catalysts preparations

$\gamma$-$Al_2O_3$ from Across (88 $m^2$/g BET surface area) was impregnated with $Cu(NO_3)_2 \cdot 3H_2O$ water solutions ($10\,ml_{solution}/g_{Al_2O_3}$) of the required concentration to obtain catalysts with different target copper loading (1, 3, 5, 7, 10 and 15 wt.%). The solvents was removed by air bubbling, and once apparently dry, the samples were heated in static air at 110 °C for 12 h and calcined at 700 °C for 5 h for nitrate decomposition. The calcination temperature has been selected taking into account that the complete soot conversion in the catalytic tests performed with $NO_x/O_2$ is reached at 700 °C. The catalysts are denoted by "Cu_X%", where "X" indicates the target copper loading.

### 2.2. Catalyst characterizations

The catalysts BET surface areas were determined by physical adsorption of $N_2$ at −196 °C in an automatic volumetric system (Autosorb-6B from Quantachrome) after degassing the samples at 250 °C for 4 h.

The actual copper loading (Cu(%)) of the different catalysts was determined by ICP in a Perkin–Elmer device, model Optimal 3000. For this purpose, the metal was extracted from the catalysts (after mechanical vibration using an ultrasonic bath to remove weakly attached metal particles) by refluxing them in a 6 M HCl solution for 8 h.

X-ray diffractograms of the catalysts were recorded in a Seifert powder diffractometer, using CuK$\alpha$ radiation. Spectra were registered between 20 and 80° ($2\theta$) with a step of 0.02° and a time per step of 3 s.

Temperature Programmed Reduction experiments were carried out with $H_2$ (TPR-$H_2$) in a Micromeritics device, model Pulse ChemiSorb 2705. 20 mg of catalyst were heated at 10 °C/min from 25 to 900 °C under a 5% $H_2$/Ar flow (35 ml/min, $P_{total}$ = 1 atm), and the $H_2$ consumption was monitored with a TCD detector. A CuO reference sample (supplied by Micromeritics) has been used to quantify $H_2$ consumption.

The Micromeritics device was also used for the estimation of copper dispersion, following the procedure described by Gervasini and Bennici [17]. The method consists of, firstly, the copper oxide reduction with 5% $H_2$/Ar (15 ml/min) by heating 150 mg of catalyst at 8 °C/min from 25 to 400 °C, holding the maximum temperature for 30 min. Then, the selective oxidation of the copper surface to $Cu_2O$ is performed under 0.53% $N_2O$/Ar flow (20 ml/min) at 50 °C:

$$N_2O + 2Cu_{surface} \rightarrow Cu_2O_{surface} + N_2 \tag{1}$$
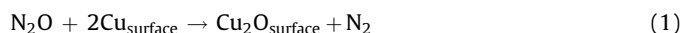
$Cu_2O_{surface}$ is further reduced with 5% $H_2$/Ar (15 ml/min) by raising the temperature at 20 °C/min from 25 to 1050 °C, following the $H_2$ consumption with the TCD detector.

$$H_2 + Cu_2O_{surface} \rightarrow 2Cu_{surface} + H_2O \tag{2}$$
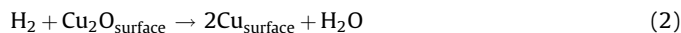
Surface copper is determined considering the stoichiometry of the reaction (2), and the parameter "Dispersion (%)" is calculated as the ratio between the amount of surface copper and total copper measured by ICP.

$$Dispersion(\%) = \frac{Cu_{surface}(g)}{Cu_{total}(g)} \times 100 \tag{3}$$

Once copper loading and dispersion were determined, the surface copper of the catalysts ($Cu_{surface}$ (%)) was estimated with the Eq. (4):

$$Cu_{surface}(\%) = \frac{Cu_{surface}(g)}{Mass\ of\ catalyst(g)} \times 100$$
$$= \frac{Dispersion(\%) \cdot Cu(\%)}{100} \tag{4}$$

XPS characterization was carried out in a VG-Microtech Multilab electron spectrometer using Mg-K$\alpha$ (1253.6 eV) radiation source. To obtain the XPS spectra, the pressure of the analysis chamber was maintained at $5 \times 10^{-10}$ mbar. The binding energy (BE) scale was adjusted by setting the C1s transition at 284.6 eV.

### 2.3. Catalytic tests

Catalytic tests were performed in a fixed-bed reactor at atmospheric pressure under a gas flow (500 ml/min) containing synthetic air or 500 ppm $NO_x$ + 5% $O_2$. The model soot used was a carbon black from Cabot (Vulcan XC72). The experiments consisted of heating the soot-catalyst mixtures from 25 to 800 °C at 10 °C/min. The soot-catalyst mixtures contained 80 mg of catalyst +20 mg of soot +300 mg SiC, and were prepared with a spatula following the so-called "loose contact" procedure [18]. Blank experiments were performed only with the catalysts (without soot) under similar experimental conditions. The gas composition

was monitored by specific NDIR-UV (Non-Dispersive Infrared Ultra-Violet) gas analyzers for NO, $NO_2$, CO, $CO_2$ and $O_2$ and the soot conversion was determined from CO and $CO_2$ evolved.

$$-\frac{dm}{dt} = (CO + CO_2) \cdot F \qquad (5)$$

In the Eq. (5), "$m$" is the mass of soot, "$t$" the reaction time, CO and $CO_2$ the volumetric fraction of each gas, and $F$ the total gas flow. In all the experiments, the carbon mass balance was obtained by numerical integration of Eq. (5) and was closed in the range 100–125% of the amount of soot loaded into the reactor. From soot conversion profiles, the parameter "$T50\%$ (°C)" has been determined, which is the temperature required to reach 50% soot conversion. In addition, the selectivity towards $CO_2$ formation with regard to total $CO_x$ emitted was determined by the Eq. (6):

$$CO_2\,selectivity(\%) = 100 \cdot CO_2/(CO + CO_2) \qquad (6)$$

The $N_2O$ formation as $NO_x$ reduction product was ruled out in additional experiments followed by gas chromatography using a HP 6890 plus series device. This set-up is described in detail elsewhere [19].

## 3. Results and discussion

### 3.1. Characterization of catalysts: copper loading and dispersion

Table 1 compiles the BET surface area of the different samples along with their copper loading and dispersion, as well as the percentage of copper oxide reduced during TPR-$H_2$ experiments (to see below). The BET values decrease progressively, as the copper loading increases, from 88 $m^2/g$ for the bare support to 70 $m^2/g$ for the catalyst with the highest copper loading. This is an evidence of the partial blocking of the support surface by copper. As expected, the copper dispersion decreases by increasing copper loading, that is, the particle size of copper increases.

In the Fig. 1a, the actual copper loading, as measured by ICP (Cu(%)), is drawn as a function of the target copper loading. All the catalysts contain a lower amount of copper than that expected (target copper loading), that is, values are below the auxiliary line with slope = 1. This means that part of the copper used for the impregnation is not incorporated to the alumina. It has to be underline that the Cu ICP measures was carried out after removing metals particle weakly attached, as indicated in section 2. The discrepancy between actual and target copper loading is little for catalysts till 7% loading, but there is a threshold around 9% loading that can not be overcome. It is important to mention that the sample Cu_15% shows heterogeneous appearance, and two types of particles (black and grey, respectively) can be distinguished. We attributed this fact to the presence of copper/copper oxide particles along with the copper-containing $Al_2O_3$ particles. Due to this

**Table 1**
Samples characterization

| Sample | BET ($m^2/g$) | Cu (%) | Dispersion (%) | Copper reduced in TPR-$H_2$ (%)[a] |
|---|---|---|---|---|
| $Al_2O_3$ | 88 | – | – | – |
| Cu_1% | 85 | 0.6 | 76 | 49 |
| Cu_3% | 82 | 2.3 | 59 | 100 |
| Cu_5% | 80 | 4.6 | 52 | 98 |
| Cu_7% | 78 | 6.5 | 30 | 92 |
| Cu_10% | 72 | 8.8 | 16 | 100 |
| Cu_15% | 70 | 9.4 | 14 | – |

[a] It has been assumed that Cu(II) reduction is according to the reaction $CuO + H_2 \rightarrow Cu + H_2O$
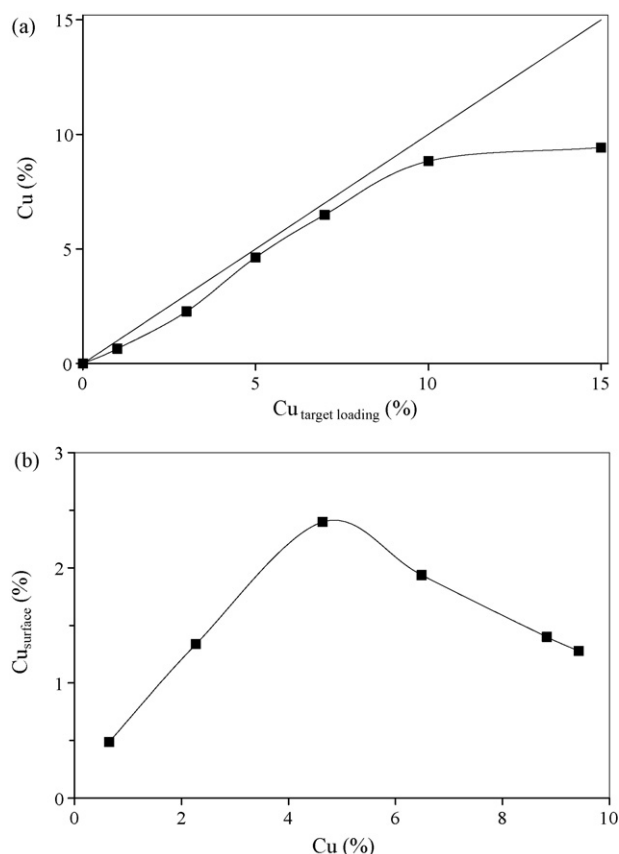


**Fig. 1.** (a) Relationship between target and actual (ICP-measured) copper loading (Cu(%)) and (b) surface copper as a function of actual copper loading (Cu(%)).

heterogeneity and lack of reproducibility in the preparation, this sample has been rejected for the catalytic tests.

One important feature of a catalyst is the surface population of active sites, which is related with the amount of surface copper on the catalyst. As expected, data in Table 1 show that the copper loading and dispersion follow opposite trends, that is, the higher the copper loading, the lower the copper dispersion. In the Fig. 1b, the surface copper is plotted as a function of the copper loading, showing an optimum value around 5% for which a maximum percentage of surface copper is reached.

In the Fig. 2, the X-ray powder diffraction patterns of the catalysts are shown. All the XRD patterns show broad diffraction
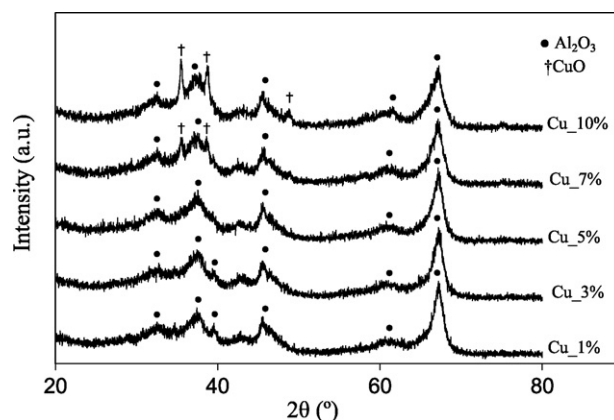


**Fig. 2.** XRD patterns of the Cu/$Al_2O_3$ catalysts.

**Table 2**
Temperature for 50% soot conversion (T50% (°C)) and $CO_2$ selectivity (%) in catalytic tests under air and $NO_x/O_2$ mixture

| Catalyst | T50% (°C) reaction under air | $CO_2$ selectivity (%) reaction under air | T50% (°C) reaction under $NO_x/O_2$ | $CO_2$ selectivity (%) reaction under $NO_x/O_2$ |
|---|---|---|---|---|
| None | 715 | 36 | 665 | 36 |
| Cu_1% | 692 | 95 | 650 | 100 |
| Cu_3% | 679 | 100 | 623 | 100 |
| Cu_5% | 666 | 100 | 610 | 100 |
| Cu_7% | 665 | 100 | 596 | 100 |
| Cu_10% | 664 | 100 | 600 | 100 |

peaks due to poorly microcrystalline γ-alumina. The diffraction peaks corresponding to copper-containing phases are not observed for Cu_1%, Cu_3% and Cu_5% catalysts, in agreement with the high copper dispersion, while the most intense reflections corresponding to CuO (at 2θ values of 35.5° and 38.8°) are clearly visible for the catalysts Cu_7% and Cu_10%. The presence of metal oxide clusters with a strong interaction with the support cannot be excluded because their XRD diffraction peaks appear at the same 2θ angles that those of $Al_2O_3$. The absence of CuO diffraction peaks in some catalysts indicate the formation of finely dispersed copper species on the alumina surface that are not detectable by this technique. Thus, XRD results are in agreement with copper dispersion results.

In conclusion, the results discussed in this section indicate that the highest surface copper amount is reached with 5% copper loading, and with the experimental procedure followed and materials used, it is not possible to reach copper loading higher than 9%.

### 3.2. Catalytic tests in air

In the Fig. 3, the soot conversion profiles during soot oxidation experiments in air are plotted as a function of temperature and, in the Table 2, the values of the parameter T50% are compiled together with those of $CO_2$ selectivity determined with the Eq. (6).

The onset temperature for the uncatalysed combustion in air is 600 °C approximately, and the complete conversion is reached at 775 °C. All the catalysts tested increase the soot combustion rate and shift the conversion profiles to lower temperatures. The catalytic activity increases with the copper loading from Cu_1% to Cu_5%, but higher copper loading do not improve the catalytic activity. According to these results, it does not make sense to increase the copper loading above 5% for soot oxidation in air. Considering the characterization results discussed in the previous section, the activity in air cannot be directly correlated with the copper loading and neither with the surface copper (Fig. 1b), because there are catalysts with the same activity but different

surface copper (Cu_5%, Cu_7% and Cu_10%). The main characteristic of the copper catalysts affecting their activity in air will be explained in detail afterwards, in section 3.4, focussed on TPR-$H_2$ and XPS characterization.

On the other hand, all the copper catalysts improve the selectivity towards $CO_2$ formation from 36% for the uncatalysed reaction to about 100% for all the copper-catalysed reactions (data in Table 2). Note that $CO_2$ is the desired soot oxidation product due to the high toxicity of CO. This improvement in $CO_2$ selectivity could be attributed, in one hand, to the fact that soot combustion takes place at lower temperature, and CO is the thermodynamically preferred product at high temperature. However, the difference between $CO_2$ selectivity for the uncatalysed (36%) and catalysed reactions (~100%) is too high considering the relatively narrow range of temperatures (600–775 °C) where soot combustion takes place. Therefore, even if the decrease in soot oxidation temperature could affect in some extent the $CO_2$ selectivity data, it is not the main argument to justify these values. On the other hand, copper-catalysts are active for CO oxidation to $CO_2$, and this seems to be the main reason of the high selectivity of the catalysts studied towards $CO_2$ formation. Thus, CO seems to be the primary soot oxidation product, as deduced from the uncatalysed experiments and copper catalyses the oxidation of CO to $CO_2$ afterwards. The high activity of copper for CO oxidation is well known, and some authors have proposed Cu-based catalysts as potential candidates to substitute precious metals in CO oxidation catalysts [20].

### 3.3. Catalytic tests in $NO_x/O_2$

#### 3.3.1. Soot oxidation

The effect of $NO_x$ in soot oxidation has been studied, and the Fig. 4 shows the soot conversion profiles during the experiments performed under $NO_x/O_2$. In the presence of $NO_x$, the uncatalysed and copper-catalysed reactions take place at lower temperatures than the counterpart reactions in air (Fig. 3). Considering the T50% temperatures included in Table 2, there is a shift of around
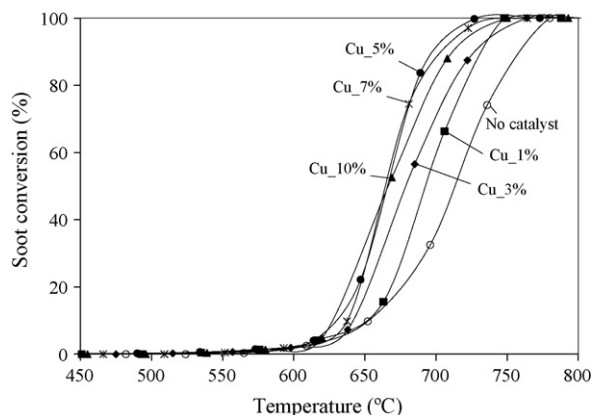

Fig. 3. Soot conversion profiles in catalytic tests performed under air.
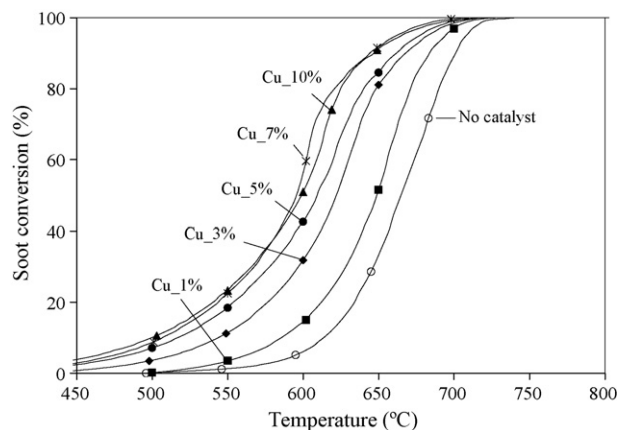

Fig. 4. Soot conversion profiles in catalytic tests performed under $NO_x/O_2$.

50 °C to lower temperature in $NO_x/O_2$ in comparison to air. The shift in the light-off temperatures for the catalysed reactions is greater, being around 500 °C for most of the copper-catalysed reactions in $NO_x/O_2$.

Copper loading also has a significant effect on catalytic activity in $NO_x/O_2$, as described for air. For instance, the T50% values (Table 2) decrease progressively from 650 to 596 °C from Cu_1% to Cu_7%, respectively. Above this loading there is not additional increase in activity, Cu_7% and Cu_10% showing quite similar behaviour. The catalytic activity of copper in $NO_x/O_2$ can not be correlated with one of the single parameters described in section 3.1 (copper loading, copper dispersion or surface copper), as already discussed for experiments in air, and some other characteristic seems to play the major role. This will be discussed afterwards.

The copper catalysts are also selective for $CO_2$ formation as soot oxidation product in the presence of $NO_x$ (data in Table 2). In fact, CO emission is not detected in any catalytic tests performed under $NO_x/O_2$. This is not the case of the uncatalysed reactions, where the same low $CO_2$ selectivity (36%) is obtained both under air and $NO_x/O_2$, supporting that copper is responsible of the high $CO_2$ selectivity.

### 3.3.2. $NO_x$ removal

The $NO_x$ removal profiles obtained during the soot oxidation tests are compiled in the Fig. 5a, and for proper interpretation of these profiles, the counterpart curves obtained in blank experiments (without soot, only using the catalysts) have been included in the Fig. 5b.

The uncatalysed soot oxidation in $NO_x/O_2$ takes place between 500 and 725 °C approximately (see Fig. 4). In this range of



temperature $NO_x$ removal occurs, as observed in the Fig. 5a, due to the $NO_x$–C reaction that yields $N_2$ and $CO/CO_2$. This reaction takes place simultaneously to the $O_2$–C combustion, which is the main soot consumption pathway. For the sake of brevity, the $O_2$ consumption profiles are not shown.

$NO_x$ removal profiles in catalytic combustion experiments are much more complexes than soot oxidation profiles. Regardless the catalyst considered, all the $NO_x$ removal profiles reach a maximum value in the range 600–700 °C that must be attributed to $NO_x$ reduction by soot. The temperature for this maximum $NO_x$ removal decreases as the copper loading increases from Cu_1% to Cu_5%, and it is reached more or less at the same temperature for Cu_5%, Cu_7%, and Cu_10%. This trend is consistent with the trend in soot conversion temperature (see soot conversion profiles in Fig. 4 and T50% values in Table 2). The maximum $NO_x$ reduction level reached was 11% (for Cu_1%), and therefore, the $Cu/Al_2O_3$ catalysts studied could not be used for the simultaneous removal of $NO_x$ and soot without an additional $NO_x$ removal strategy.

The $NO_x$ removal profiles obtained with Cu_5%, Cu_7%, and Cu_10% also show a wide shoulder at lower temperatures (around 450 °C), which must be attributed to $NO_x$ chemisorption on the catalysts. It is reasonable to assume that between both ranges of temperature (shoulder around 450 °C and maximum at 600–700 °C), both processes ($NO_x$ chemisorption and $NO_x$ reduction, respectively) could progress together.

The hypothesis of $NO_x$ chemisorption on the catalysts around 450 °C was confirmed in experiments performed without soot (Fig. 5b), since in this case the $NO_x$ removal pathway throughout the $NO_x$–C reaction can be ruled out. $NO_x$ removal in blank experiments (without soot) due to chemisorption on the catalysts depends on the copper loading, increasing from Cu_1% to Cu_5% with maximum removal for the latter, and slightly decreasing for Cu_7% and Cu_10%. This trend is the same than that obtained for surface copper in the Fig. 1b, and indicates that $NO_x$ chemisorption, as expected, is a surface phenomenon.

Comparison between Fig. 5a and b allows concluding that the copper-catalysed soot combustion decreases the amount of $NO_x$ chemisorbed on the catalyst. As an example, $NO_x$ removal on the Cu_5% catalyst reaches 15% at 450 °C in the absence of soot (Fig. 5b) while the $NO_x$ removal in the presence of soot at the same temperature is only 3% for this catalyst. This is because the copper surface is involved in both the $NO_x$ chemisorption and the catalysed soot oxidation, and therefore, it is expected that the copper fraction involved in the catalysed soot oxidation is not available for $NO_x$ chemisorption. The same phenomenon was previously observed for a $CeO_2$ catalyst [21]. Related with this fact, Pisarello et al. [22] also concluded that the formation of stable nitrate species on a $K/Ba/CeO_2$ catalyst inhibits the soot combustion reaction.

One important issue that must be considered in catalysed soot oxidation under $NO_x/O_2$ is the formation of $NO_2$, which is much more oxidising than NO and $O_2$, as mentioned. NO is the main component of $NO_x$ in a real diesel exhaust, and it is also in the experimental set-up used for the catalytic tests. In the Fig. 6, the $NO_2$ percentage, on the basis of the NO + $NO_2$ level, is plotted as a function of temperature for the blank experiments. Despite $NO_2$ is the thermodynamically stable nitrogen oxide at low temperature, the conversion of NO to $NO_2$ presents kinetic restrictions, and the copper catalysts raise the NO oxidation rate. For instance, $NO_2$ is detected from 300 °C with the catalyst Cu_10%, reaches a maximum level of 14% at 465 °C, and then decreases following thermodynamics. The delay between thermodynamics and experimental $NO_2$ profiles must be attributed to the time required for the gas to go from the reactor to the analysers. The maximum $NO_2$ concentration reached depends on the copper loading, and as a
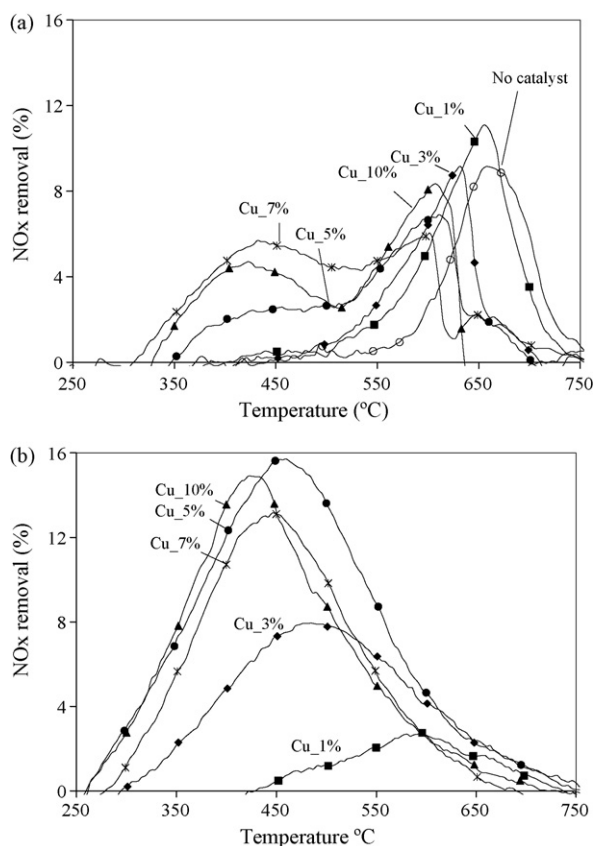
**Fig. 5.** $NO_x$ removal profiles in catalytic tests performed under $NO_x/O_2$. (a) With soot and (b) without soot (blank experiments).
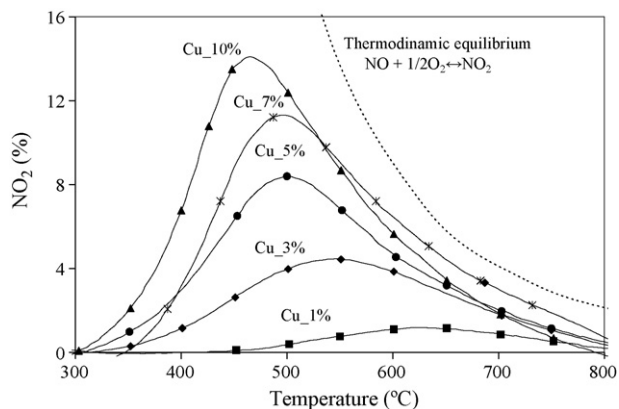
Fig. 6. $NO_2$ percentage in catalytic tests performed under $NO_x/O_2$ without soot.



Fig. 8. Catalysts characterization by TPR-$H_2$.

general trend, the higher the loading the higher the activity for NO oxidation to $NO_2$. These results suggest that there is a certain relationship between the catalytic activity of the copper catalysts for NO oxidation to $NO_2$ and for soot oxidation, which is due to the high soot oxidation capacity of $NO_2$. For example, the trend in $T50\%$ temperatures (Table 2) for Cu_1%, Cu_3% and Cu_5% (650, 623, and 610 °C, respectively) is related to the trend of the maximum $NO_2$ level reached in Fig. 6 (1, 4, and 8%, respectively).

However, it is surprising that the catalytic activity for soot combustion of Cu_7% and Cu_10% are almost the same (see profiles on Fig. 4 and $T50\%$ values on Table 2) while the latter is much more effective for $NO_2$ formation (Fig. 6). This could be attributed to the fact that the maximum $NO_2$ level is reached around 450 °C for both catalysts, and the reactivity of soot at this temperature is low (Fig. 4). In other words, $NO_2$ is not effective for soot oxidation at 450 °C, at least for the model soot used in this study. Most probably, the rate limiting step at 450 °C is the decomposition of the oxygen complexes formed on the soot surface upon $NO_2$ oxidation, but not the oxidation of the carbon surface by $NO_2$.

The relationship between the temperature required by each catalyst to reach the maximum $NO_2$ level in blank experiments (Fig. 6) and the $T50\%$ temperatures determined in the catalytic tests (Table 2) is depicted in Fig. 7. Previous discussion is confirmed; a linear trend is observed for Cu_1%, Cu_3% and Cu_5%. In this case, the soot oxidation depends directly on the $NO_2$ production, which is kinetically controlled by the catalysts. For the catalysts Cu_7% and Cu_10% this trend is not followed because of the low reactivity of the model soot at the temperature of maximum $NO_2$ production. In fact, it has been probed that using a
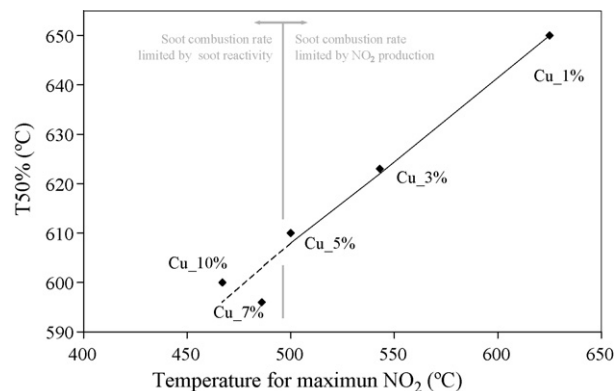


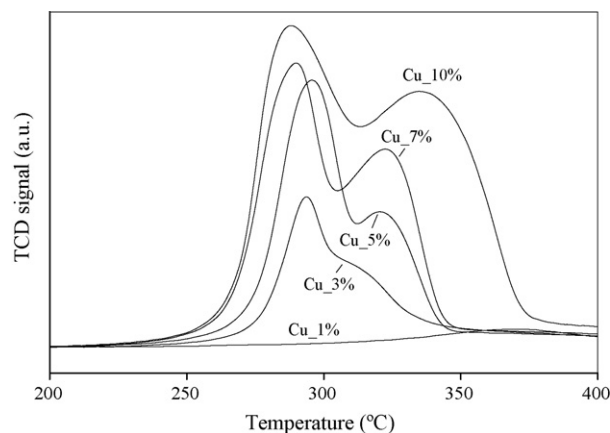Fig. 7. Relationship between temperature of maximum $NO_2$ formation and $T50\%$ in catalytic tests.

more reactive model soot (Printex-U), Cu_7% and Cu_10% catalysts follow the observed trend.

### 3.4. TPR-$H_2$ and XPS characterization

In this section, the redox properties of copper are studied by TPR-$H_2$, and the surface copper species are evaluated by XPS.

The TCD signal profiles obtained in the TPR-$H_2$ experiments with the set of copper catalysts are drawn in the Fig. 8. All the catalysts consumed $H_2$ in these tests because of the reduction of copper oxide. As expected, the higher the copper loading, the higher the $H_2$ consumption. The percentage of copper oxide reduced during these experiments has been estimated from $H_2$ consumption, considering that Cu(II) is the copper specie reduced, and the data obtained are included in the Table 1. Except for Cu_1%, all the catalysts reach near 100% copper reduction. This confirms that the assumption is right and supports that Cu(II) is reduced but not Cu(I) (if Cu(I) were the main copper oxide specie, values around 50% would be expected). Additionally, it is possible to conclude that the presence of metallic copper is minor or null in all the catalysts, except in Cu_1%.

Most of the TCD signal profiles (Fig. 8) show two peaks, indicating that copper oxide species with different redox behaviour are present. A peak appears at 275 °C for most catalysts, and it can be attributed to Cu(II) species that are easily reduced. This peak is probably due to the reduction of a well-dispersed CuO phase. The maximum intensity of this peak increases significantly from Cu_1% (null) to Cu_5%, and then slightly for higher copper loading, This trend is similar to that described in the catalytic tests in air (Fig. 3), suggesting that the catalytic activity is related to the amount of Cu(II) that is easily reduced. Another peak appears above 300 °C (the right temperature depends on the copper loading) corresponding to less-reducible copper oxide. This high temperature peak can be related to the reduction of larger CuO particles. The maximum intensity of the latter peak increases with the copper loading and the sequence is different to that of the copper dispersion (see data on Table 1). Similar TPR-$H_2$ profiles of $CuO/Al_2O_3$ materials has been reported by other authors for different copper catalysts ($CuO/Al_2O_3$, $CeO_2/Al_2O_3$, $Cu/CeO_2-Al_2O_3$) [24] who suggested that the redox properties of CuO are affected by the interaction with alumina and that small CuO clusters and/or isolated $Cu^{2+}$ ions are reduced at lower temperature than larger CuO particles [25].

It is important to take into account that, considering the percentage of copper reduced in TPR-$H_2$ experiments (data in Table 1), the catalyst Cu_1% could also contain a certain amount of metallic copper along with the copper oxide species. The metallic
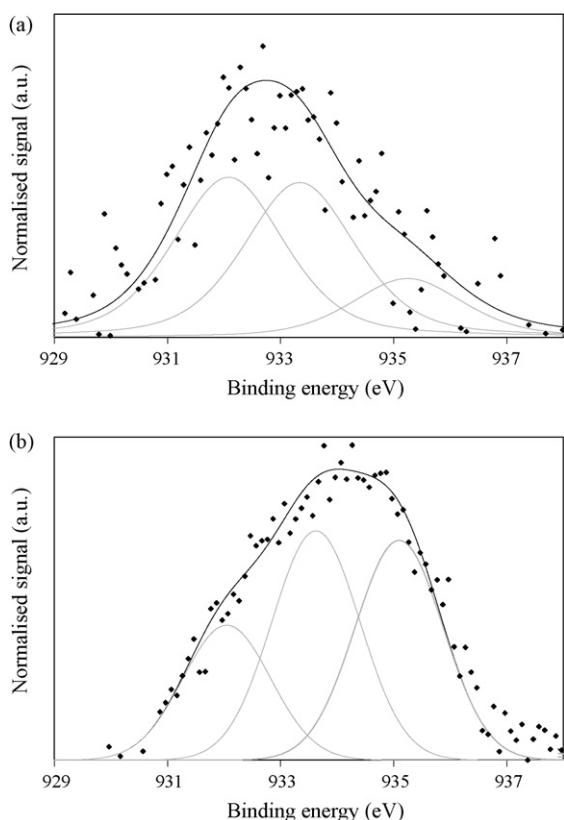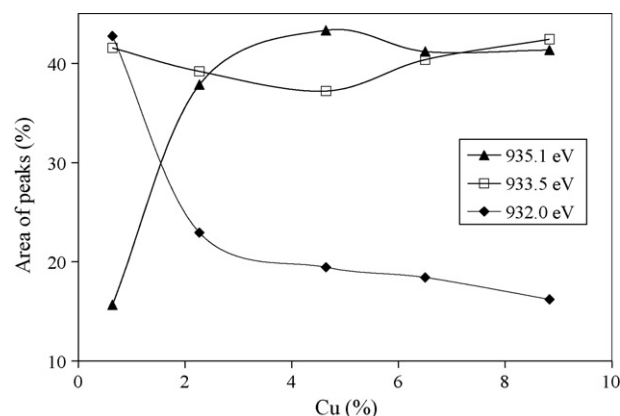
Fig. 10. Quantification of the different copper species from the deconvoluted XPS-peak areas as a function of actual copper loading (Cu(%)).

appreciated in Fig. 10 among them. All the catalysts, except Cu_1%, present around 80% CuO, calculated as the sum of the 933.5 eV and 935.1 eV contributions. This confirms that there is not important missing information in the TPR-$H_2$ profiles due to the presence of significant amounts of reduced copper species.

As a summary, the results presented in this study allow concluding that the most active copper species for catalytic soot oxidation in air is the easily-reduced Cu(II) species, which is reduced around 275 °C under TPR-$H_2$ conditions. On the contrary, less reducible Cu(II) (reduced under TPR-$H_2$ conditions above 300 °C) and reduced copper species present lower activity. The amount of the most active Cu(II) species increases significantly with the copper loading from Cu_1% to Cu_5% and slightly for higher copper loading. This is consistent to the catalytic activity trend for soot oxidation in air, and supports the hypothesis of the redox mechanism. In the presence of $NO_x$, the mechanism is more complicated. The first step seems to be the NO conversion to $NO_2$, and the catalytic activity for this reaction depends on the copper loading. For catalysts with copper loading between Cu_1% and Cu_5%, the catalytic activity for soot oxidation in the presence of $NO_x$ depends on $NO_2$ formation, and $NO_2$ formation is kinetically controlled by these catalysts. For catalysts with higher copper loading this trend is not followed because of the low reactivity of the model soot used at the temperature of maximum $NO_2$ production.

## 4. Conclusions

In this study, $Cu/Al_2O_3$ catalysts have been prepared by wet impregnation, characterized, and tested for soot combustion in air and $NO_x/O_2$, and conclusions can be summarised as follows:

- The activity of the copper catalysts for soot oxidation in air depends on the amount of easily-reduced Cu(II) species, which are reduced around 275 °C under TPR-$H_2$ conditions. The amount of the most active Cu(II) species increases significantly with the copper loading from Cu_1% to Cu_5% and slightly for higher copper loading.
- In the presence of $NO_x$, the first step of the mechanism seems to be the NO oxidation to $NO_2$, and the catalytic activity for this reaction depends on the copper loading. For catalysts with copper loading between Cu_1% and Cu_5%, the catalytic activity for soot oxidation in the presence of $NO_x$ depends on $NO_2$ formation. For Cu_7% and Cu_10% this trend is not followed because of the low reactivity of the model soot used at the temperature of maximum $NO_2$ production.



Fig. 9. XPS characterization of the Cu $2p^{3/2}$ transition for the catalysts (a) Cu_1% and (b) Cu_3%.

copper would not contribute to the TCD signal in TPR-$H_2$ experiments since it would be already reduced. In order to analyse this possibility, the catalysts surface was characterized by XPS following the Cu $2p^{3/2}$ transition. As an example, the profiles corresponding to the catalysts Cu_1% and Cu_3% are included in the Fig. 9a and b, respectively. The broad profiles can be deconvoluted in three different peaks with maxima at 932.0, 933.5 and 935.1 eV. Reduced copper species, such as metallic copper and $Cu_2O$, usually appear below 933 eV and CuO typically appears with binding energies higher than 933 eV [23]. The identification of two different CuO species by XPS (at 933.5 eV and 935.1 eV) is consistent with the TPR-$H_2$ profiles (Fig. 8), where two copper oxide species with different reducibility are also identified.

The copper species distribution is different for each catalyst. For instance, the area of the peak at 935.1 eV is low for Cu_1% (Fig. 9a) while the area of the peak at 932.0 eV is low for Cu_3% (Fig. 9b). This means that copper on Cu_1% is more reduced than on Cu_3%. In order to analyse these differences, the area under the different peaks has been quantified for all the catalysts, and the corresponding percentages have been then calculated as a function of the total area of the $2p^{3/2}$ transition profiles. In the Fig. 10, these percentages are drawn against the copper loading of the catalysts. As mentioned, Cu_1% presents the highest contribution of the most reduced copper species, with 43% of copper appearing with binding energy at 932.0 eV and only 16% with binding energy at 935.1eV corresponding to the most oxidised copper specie. This explains the low intensity of the TCD signal obtained in the TPR-$H_2$ experiment of Cu_1% (Fig. 8), and the low percentage of copper reduced in this catalyst (Table 1). In the catalyst Cu_1%, copper is quiet reduced and it does not consume $H_2$. With the only exception of Cu_1%, the remaining catalysts present quite similar surface copper species distribution, and not significant differences are

                    *F.E. López-Suárez et al. / Applied Catalysis B: Environmental 84 (2008) 651–658*

- A certain $NO_x$ reduction occurs along with the copper-catalysed soot combustion, but the maximum reduction level reached with the studied catalysts was 11%, not being high enough for a practical use.
- All the copper catalysts tested improved the selectivity towards $CO_2$, as soot oxidation product, from 36% for the uncatalysed reaction to 100% for the catalysed reactions. This behaviour is observed both under air and $NO_x/O_2$.

## Acknowledgements

## References

[1] M.V. Twigg, Appl. Catal. B 70 (2007) 2–15.
[2] A. Bueno-López, J.M. Soriano-Mora, A. García-García, Catal. Commun. 7 (2006) 678–684.
[3] R.L. Bloom, N.R. Brunner, S.C. Schroeer, SAE paper 970180, 1997.
[4] G. Mu1, F. Kapteijn, J.A. Moulijn, Appl. Catal. B 12 (1997) 33–47.
[5] X. Wu, Q. Liang, D. Weng, Z. Lu, Catal. Commun. 8 (2007) 2110–2114.
[6] Y. Teraoka, K. Kanada, H. Furukawa, I. Moriguchi, S. Kagawa, Chem. Lett. 7 (2001) 604–605.
[7] C. Badini, G. Saracco, V. Serra, Appl. Catal. B 11 (1997) 307–328.
[8] R. Cousin, S. Capelle, E. Abi-Aad, D. Courcot, A. Aboukaïs, Appl. Catal. B 70 (2007) 247–253.
[9] V.S. Braga, F.A.C. Garcia, J.A. Dias, S.C.L. Dias, J. Catal. 247 (2007) 68–77.
[10] X. Peng, H. Lin, W. Shangguan, Z. Huang, Catal. Commun. 8 (2007) 157–161.
[11] S. Wisniewski, J. Belkouch, L. Monceaux, C. R. Acad. Sci. Paris, Serie IIc, Chimie: Chemistry 3 (2000) 443–450.
[12] H. Laversin, D. Courcot, E.A. Zhilinskaya, R. Cousin, A. Aboukaïs, J. Catal. 241 (2006) 456–464.
[13] N. Nejar, M.J. Illán-Gómez, Appl. Catal. B 70 (2007) 261–268.
[14] N. Nejar, M.J. Illán-Gómez, Catal. Today 119 (2007) 262–266.
[15] S. Mosconi, I.D. Lick, A. Carrascull, M.I. Ponzi, E.N. Ponzi, Catal. Commun. 8 (2007) 1755–1758.
[16] M.J. Illán-Gómez, E. Raymundo-Piñero, A. García-García, A. Linares-Solano, C. Salinas-Martínez de Lecea, Appl. Catal. B 20 (1999) 267–275.
[17] A. Gervasini, S. Bennici, Appl. Catal. A 281 (2005) 199–205.
[18] J.P.A. Neeft, O.P. van Pruissen, M. Makkee, J.A. Moulijn, Appl. Catal. B 12 (1997) 21–31.
[19] A. Bueno-López, J.A. Caballero, A. García-García, Energy Fuels 16 (2002) 1425–1428.
[20] F.H.M. Dekker, M.C. Dekker, A. Bliek, F. Kapteijn, J.A. Moulijn, Catal. Today 20 (1994) 409–422.
[21] I. Atribak, I. Such-Basáñez, A. Bueno-López, A. García-García, J. Catal. 250 (2007) 75–84.
[22] M.L. Pisarello, V. Milt, M.A. Peralta, C.A. Querini, E.E. Miró, Catal. Today 75 (2002) 465–470.
[23] http://www.lasurface.com.
[24] E. Moretti, M. Lenarda, L. Storaro, A. Talon, T. Montanari, G. Busca, E. Rodríguez, A. Jimeénez, M. Turco, G. Bagnasco, Appl. Catal. A 335 (2008) 46–55.
[25] J.Z. Shyu, W.H. Weber, H.S. Ghandi, J. Phys. Chem. 92 (1988) 4964.